N O T I C E

THIS DOCUMENT HAS BEEN REPRODUCED FROM MICROFICHE. ALTHOUGH IT IS RECOGNIZED THAT CERTAIN PORTIONS ARE ILLEGIBLE, IT IS BEING RELEASED IN THE INTEREST OF MAKING AVAILABLE AS MUCH INFORMATION AS POSSIBLE

AN ANALYTICAL STUDY OF NITROGEN OXIDES AND CARBON MONOXIDE EMISSIONS IN HYDROCARBON COMBUSTION WITH ADDED NITROGEN — PRELIMINARY RESULTS

David A. Bittker
National Aeronautics and Space Administration
Lewis Research Center

AN ANALYTICAL STUDY OF NITROGEN OXIDES AND CARBON MONOXIDE

EMISSIONS IN HYDROCARBON COMBUSTION WITH ADDED

NITROGEN - PRELIMINARY RESULTS

by David A. Bittker

National Aeronautics and Space Administration
Lewis Research Center
Cleveland, Ohio

INTRODUCTION

One of the major efforts in the development of gas turbines for ground power generation is their adaptation to the use of coal-derived liquid fuels. The wide range of properties of these synthetic liquid fuels leads to many problems. A recent summary of coal derived liquid fuel properties and their potential problems in turbine combustion is given in Ref. 1. The present paper focuses on the problem of increased emissions. The main question is how much the oxides of nitrogen (NO_x) emissions will be increased by the increased amount of organic nitrogen compounds contained in these synthetic liquids. Another question is whether this fuel-bound nitrogen (FBN) will have any significant effect upon the carbon monoxide (CO) emissions from synthetic fuel combustion.

The present work was undertaken to investigate these questions as one part of the Critical Research and Technology program funded by the Department of Energy at the Lewis Research Center. The primary purpose of this work is to analytically determine the effect of combustion operating conditions on the conversion of FBN to NO_x. The effect of FBN and of operating conditions on CO emissions was also examined. Propane-air was chosen as the combustible mixture for the first series of computations. The combustor model was assumed to be a two-stage, adiabatic, perfectly-stirred reactor. Chemical modeling of the oxidation of propane and the formation of NO_x was done using a fifty-seven reaction mechanism. The use of two-stage combustion to minimize NO_x formation has been reported by several investigators (2 to 4).[1] The greatest NO_x

---

[1]Numbers in parentheses designate references at end of paper.

reduction is achieved by burning with a rich primary mixture and then diluting with air for quite lean second-stage combustion.
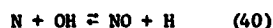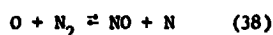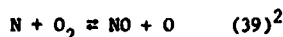
A wide range of operating conditions was used for these computations. Primary equivalence ratio, φ_p, was varied from 0.5 to 1.7. Dilution air was added in the secondary zone, as necessary, to give a secondary equivalence ratio, φ_s, of either 0.5 or 0.7. Primary stage residence time varied from approximately 12 to 20 msec and secondary stage residence times of approximately 1, 2, and 3 msec were used. Three different amounts of FBN were used in the computations, namely 0.5, 1.0, and 2.0 percent by weight of the initial fuel. All computations were performed for a constant pressure of 5 atm and initial mixture temperatures ranged from 608 to 650 K.

Computations were performed using the NASA Lewis General Chemical Kinetics Program (5), which was modified to perform stirred-reactor model computations. The nonlinear algebraic equations given in Refs. 6 and 7 for multicomponent, chemically rate-limited homogeneous reaction in a perfectly-stirred reactor were used. Solution of these equations by the modified Newton-Raphson iteration procedure given in Ref. 6 was programmed and incorporated as a subroutine into the general chemical kinetics program.

Results are presented for NO_x and CO concentrations as a function of φ_p, φ_s and both primary and secondary residence times, as well as the amount of FBN. A limited comparison of the computed results with experimental results obtained under another task in the Critical Research and Technology program is also given. The comparison will show the good semi-quantitative agreement between our theoretical model and the experimental results. It should be mentioned that neither the theoretical computations nor the experimental work were meant to model a practical turbine combustor.

Moreover, the effects of initial temperature and pressure variation were considered of secondary importance. These conditions were not changed in either the experimental or the theoretical work.

The chemistry of nitrogen oxide formation during combustion has been studied extensively for many years. Two good reviews of this topic are given in Refs. 8 and 9. In this paper we shall define nitrogen oxides or NO_x as the sum of nitric oxide (NO) and nitrogen dioxide (NO_2) concentrations. Although the mechanism of NO_x formation in lean hydrocarbon combustion is fairly well known, our knowledge is still lacking for very rich mixtures (i.e., equivalence ratios from about 1.2 to 2). For lean combustion NO_x formation is explained mainly by the extended Zeldovich mechanism

$$N + O_2 \rightleftarrows NO + O \qquad (39)^2$$

$$O + N_2 \rightleftarrows NO + N \qquad (38)$$

$$N + OH \rightleftarrows NO + H \qquad (40)$$

and the additional reaction:

$$O + NO_2 \rightleftarrows NO + O_2 \qquad (31)$$

To explain experimental NO_x concentrations higher than computed values for rich mixtures Fenimore (10) suggested the direct reaction of hydrocarbon fragments with molecular nitrogen:

$$CH + N_2 \rightleftarrows HCN + N \qquad (41)$$

Both products of this reaction can lead to additional NO formation. The additional reactions of HCN, CN, and NH_i species are the unknowns in the path of complete understanding of NO_x formation. Jachimowski (11) showed that the addition of only reaction (41) to the fairly well known methane oxidation mechanism improved rich combustion NO prediction considerably. And more recently, Wakelyn, Jachimowski and Wilson (12) developed a comprehensive propane-air combustion mechanism. It employs not only reaction (41) but those involving HCN, CN, NCO, and NH species. When applied to computing NO concentrations for stirred-reactor combustion of rich propane-air mixtures (up to $\varphi = 1.4$), this mechanism gave excellent agreement with experimental results obtained in their laboratory. These investigators also applied the stirred-reactor model and their propane-air chemical model in computations attempting to match experimental flame-tube emission data of Anderson (13). The computed and experimental results agreed quite satisfactorily.

In choosing the mechanism for the present computations we have, therefore, used a modification of the mechanism developed in Ref. 12. One of the key contributions of that work is the fact that the computed NO concentration is very sensitive to the rate constant, k_{41} for reaction (41). The authors used this fact to derive a new value for k_{41} which gave the best agreement between their computed and experimental results and this improved value of k_{41} was used in the present computations. The complete mechanism used in the present computations is given in Table I, along with rate constants and their sources. The first 40 reactions plus reaction 52 were sufficient for computations at φ_p values from 0.5 to 1.0. The full mechanism was used for all φ_p values greater than 1.0.

---

[2]Reactions are numbered to correspond to numbers in Table I.

In previous analytical modeling of fuel-bound nitrogen conversion to NO_x (4 and 13) the FBN has been simulated by simple species such as N, NH, NH_3, HCN, CN. This is necessary because of the complexity of the organic nitrogen compounds in synthetic fuels and the lack of detailed kinetic data on the pyrolysis of these compounds. The rationale for using one of these "model compounds" to represent FBN is detailed in Ref. 14. The basic assumption is that one of these simple species represents the major pyrolysis product of the more complicated molecule that can react to form NO_x. The work of Ref. 14 showed that computed results for NO conversion using N, NH, CN, and HCN are semiquantitatively similar. Inasmuch as our combustor model is quite idealized, we chose the simplest species, nitrogen atom, as our model compound for the FBN. It should be mentioned that using N as the model compound gives about 25 percent less conversion to NO_x than using the other model compounds. This is due to the importance of the reverse of reaction 38, $NO + N \rightarrow O + N_2$.

RESULTS AND DISCUSSION

Effect of Fuel-Bound Nitrogen

The main interest in this paper is the effect of FBN on both NO_x and CO final concentration. This effect is shown in Fig. 1 for NO_x and Fig. 2 for CO. In each figure computed final pollutant concentration, with no further dilution, is plotted against initial equivalence ratio, φ_p, from 0.5 to 1.7 for several different FBN contents. For these computations primary reaction volume was constant at 4360 cm^3, the shortest primary-zone residence time; secondary residence time was fixed at nominally 1 msec. These conditions were chosen to correspond to those used in the experimental flame tube work which will be described briefly in a following section. Secondary air was added when necessary to give a φ_s value of 0.7. Primary mixtures leaner than $\varphi_p = 0.7$ were not diluted. It is observed in Fig. 1 that the minimum NO_x concentration is always obtained at a φ_p value between 1.4 and 1.5 for the range of φ_p shown. At the φ_p value for this minimum NO_x concentration the CO concentration (Fig. 2) always attains its maximum value. Although NO_x always increases as FBN is increased, the highest percent conversion of FBN to NO_x occurs for 0.5 percent FBN at the rich φ_p values. For example, at $\varphi_p = 1.4$ the FBN conversions are approximately 25, 19, and 15 percent for initial FBN contents of 0.5, 1.0, and 2.0 percent, respectively. The decrease in FBN conversion with increased FBN content has been observed by others (14). The effect of FBN on CO formation is quite different. Figure 2 shows that any FBN decreases the final CO concentration. For $\varphi_p = 1.4$, the point of greatest CO concentration, any amount of FBN decreases the CO concentration by about 17 percent.

The effect of added FBN on final NO_x concentration can be seen better in Fig. 3 where the NO_x concentration is plotted against percent of FBN for several different primary equivalence ratios. This plot shows that the greatest percentage increase of NO_x concentration with added FBN occurs at the extremely lean and the very rich primary equivalence ratios. The absolute increase in NO_x concentration for a fixed addition of FBN does not change greatly with primary equivalence ratio. For example we can compare NO_x concentrations for 0 and for 0.5 percent FBN in the following table

φ_p	NO_x concentration, ppm		Absolute change, ppm	Percent change
	0% FBN	0.5% FBN		
0.6	155	500	345	222
.9	2130	2400	270	13
1.4	110	340	230	209

The absolute changes in NO_x concentration are between 230 and 345 ppm. But this translates to a change of about 200 percent at the highest and lowest φ_p values and a change of only 13 percent at $\varphi_p = 0.9$, where NO_x formation is highest without FBN present. Also in Fig. 3, the decrease in NO_x concentration gradient as percent FBN rises above 0.5 is particularly noticeable at $\varphi_p = 1.4$, the condition for minimum NO_x formation in general.

Effect of Secondary Dilution

The effect of additional dilution was studied by repeating the second stage computations for a φ_s value of 0.5 instead of 0.7. The results for final NO_x concentration are shown in Fig. 4 and for CO concentration in Fig. 5. All other conditions are the same as in Figs. 1 and 2. Final pollutant concentration is again plotted against φ_p for various amounts of FBN. Comparison of Figs. 4 and 1 and Figs. 5 and 2 show that the trends are very much the same. However, both pollutant concentration levels have been significantly reduced by the added dilution. For a better quantitative comparison of dilution effects we have replotted the 1 percent FBN NO_x formation curves from Figs. 1 and 4 together in Fig. 6(a). Likewise the 1 percent FBN CO formation curves from Figs. 2 and 5 are replotted together in Fig. 6(b). From these plots it is seen that the greatest percentage reduction due to additional dilution in both NO_x and CO is at a φ_p value close to 1.4, the value for minimum NO_x. NO_x is reduced by about 47 percent and CO by 57 percent due to the additional dilution.

The observed concentration reductions are, of course, the combined effect of physical dilution of the primary gas and the chemical reaction in the secondary-stage combustion. It is of interest to compare these two effects for the present model and this can be done with the help of Table II. In this table we have listed three different values of NO_x and CO concentration for several φ_p values and for secondary dilution to both $\varphi_s = 0.7$ and $\varphi_s = 0.5$. In addition to the secondary exhaust gas concentration we have listed the primary exhaust gas concentration and also the diluted primary exhaust gas concentration before the secondary chemical reaction. For NO_x the table shows that only the dilution of the primary mixture determines final concentration for the lean and stoichiometric φ_p values of 0.8 and 1.0. For both secondary dilutions the NO_x concentration is increased by at most 2 percent during the secondary reaction. For example, at $\varphi_p = 1.0$ and $\varphi_s = 0.7$ NO_x concentration increases from 2242 to 2291 ppmm during the secondary reaction. For the rich primary mixtures, however, there is significant chemical reaction forming NO_x in the secondary stage when dilution is to $\varphi_s = 0.7$. At $\varphi_p = 1.4$, for example, the secondary chemical reaction increases NO_x by 37 percent from 327 to 447 ppmm. For dilution to $\varphi_s = 0.5$ there is, however, negligible chemical reaction forming NO_x when φ_p is 1.2 and 1.4. The probable reason for this can be seen in Fig. 7, where secondary reaction temperature is plotted as a function of φ_p for both secondary dilutions. The same 1.0 percent FBN content as in Figs. 6(a) and (b) was used. The reaction temperature is reduced by more than 300 K for all φ_p values from 0.8 to 1.7 when φ_s goes from 0.7 to 0.5. This drop in temperature could easily quench the NO_x formation reactions which are very temperature dependent. The situation is quite different for CO. Table II shows that the final CO concentration is determined mainly by secondary stage chemical reaction for all conditions. This is especially true for the rich primary mixtures in which CO concentration is very high. The reason for the quite different behavior of CO concentration is the lack of temperature dependence of the main CO oxidation reaction

$$CO + OH \rightleftharpoons CO_2 + H \qquad (20)$$

A drop of 300 K in temperature, as shown in Fig. 7, has a negligible effect on the rate constant of this reaction.

Effect of Primary and Secondary Residence Times

Primary zone residence time was increased by changing the reaction volume by factors of 1.2 and 1.4. Thus a typical residence time of 12 msec at the smallest reaction volume was changed to about 17 msec for the largest volume. No significant effect on primary residence time was predicted for either pollutant. Typical examples of the variation of NO_x and CO with primary residence time are shown in Figs. 8 and 9. Pollutant concentration is plotted against primary equivalence ratio for mixtures containing 1.0 percent fuel-bound nitrogen using three different primary residence times.

All secondary-stage computations were performed using three different reaction volumes. They were chosen to give nominal secondary residence time values of 1, 2, and 3 msec. Typical plots of NO_x concentration versus secondary residence time with φ_p as a parameter are shown in Figs. 10(a) and (b). For Fig. 10(a) the secondary stage φ_s value is 0.7 and for Fig. 10(b) it is 0.5. Mixtures containing one percent FBN were used for the computations. For dilution to $\varphi_s = 0.7$, we see that the NO_x results are somewhat sensitive to residence time variation for the very rich mixtures ($\varphi_p = 1.4$ and 1.7). There is a 35 percent increase in NO_x concentration as residence time increases from 1 to 3 msec at $\varphi_p = 1.4$. When the secondary dilution is to $\varphi_s = 0.5$, however, Fig. 10(b) shows that final NO_x concentration is completely independent of secondary residence time. These results are explained by the temperature effect on NO_x forming reactions just discussed. There can only be an effect of secondary residence time on NO_x concentration where there is chemical reaction in the secondary zone. It has just been shown that NO_x concentration increases in the secondary zone only for rich mixtures diluted to $\varphi_s = 0.7$. The effect of secondary residence time on CO concentration is shown in Figs. 11(a) and (b). The plots are exactly analogous to Figs. 10(a) and (b). In contrast to NO_x, the CO concentration decreases as residence time increases for all values of φ_p and both secondary dilutions. Moreover, the rate of decrease of CO concentration with residence time is fairly independent of both primary equivalence ratio and amount of secondary dilution. The trends shown here, for 1.0 percent FBN in the fuel, are similar to those for other added amounts of FBN. When no added FBN is present, the trends are the same especially for secondary dilution to $\varphi_s = 0.5$. The only difference is observed for $\varphi_s = 0.7$. For this dilution the NO_x concentration increases more sharply with increasing secondary residence time for $\varphi_p = 1.4$ and 1.7 than shown in Fig. 10(a).

Comparison with Experimental Data

Experimental emission measurements are being made by G. Wolfbrandt and D. Schultz at the Lewis Research Center in another part of the CRT program. Their apparatus is a two-stage flame tube. A highly turbulent hydrocarbon-air mixture is burned in two stages, with dilution in the second stage exactly as described for the present idealized stirred-reactor model. Both propane-air and propane-toluene-air mixtures are being used in this program and pyridine is added to simulate fuel bound nitrogen. The purpose of this experimental work is the same as for the present theoretical study; that is, to determine the effect of operating conditions on FBN conversion to NO_x. To test whether the idealized stirred-reactor model predicts the qualitative experimental trends we have made plots comparing experimental and computed results. Figure 12 shows experimental and computed NO_x concentration vs. φ_p and Fig. 13 shows CO concentration vs. φ_p. These results are for propane-air with no added FBN. The experimental points are the first data from the flame-tube experiment. For both pollutants the qualitative agreement can be seen to be quite good. Moreover, the quantitative agreement steadily improves as we go to rich primary equivalence ratios. For this latter region agreement is within ±50 percent.

Some possible sources of discrepancy are: (1) an incomplete chemical model of the combustion; (2) experimental heat losses; and (3) mixing nonhomogeneity during the experiment.

The present chemical model should be equivalent to the model of Ref. 12 in matching the data of Anderson (13). We find this to be true when we compare the results of our primary zone computations with the experimental results of Anderson. Our computed primary zone NO_x and CO concentrations are in good agreement with Anderson's results for all equivalence ratios. Therefore the observed discrepancies between computed and experimental second-stage pollutant concentrations are probably due to mixing non-homogeneity and heat losses in the second stage combustion. One important point is the fact that there is a finite length of mixing and chemical reaction at the entrance to the secondary zone for the experiment. The computational model assumes instantaneous mixing of the dilution air with the primary exhaust gases before the secondary reaction begins. Apparently the experimental effects are less important when the primary-zone burning is rich.

SUMMARY OF RESULTS

In this study we have predicted analytically the effect of operating conditions on pollutant formation in two-stage combustion. In particular we have studied the effect of these conditions on fuel bound nitrogen conversion to NO_x and also on CO formation. Propane-air mixtures were assumed to burn in a two-stage, adiabatic, perfectly-stirred reactor. Various amounts of fuel-bound nitrogen, up to 2 percent by weight as nitrogen atoms, were used. The product gases of the primary stage were diluted by added air in the second stage to an overall equivalence ratio of either 0.7 or 0.5. The computed results were compared with a limited amount of experimental data. The important results of this work may be summarized as follows:

1. Minimum NO_x formation occurs in general when the primary zone equivalence ratio is between 1.4 and 1.5. However, for this range of values, the CO formation is at its highest level.

2. The percentage conversion of fuel bound nitrogen to NO_x is greatest for small percentages of FBN and decreases as FBN content is raised above 0.5 percent by weight.

3. The final concentrations of NO_x and CO are significantly reduced by additional secondary dilution from $\varphi_s = 0.7$ to $\varphi_s = 0.5$. The extra dilution lowers the secondary reaction temperature by about 300 K and thus suppresses all secondary-stage NO_x reactions. Therefore, the change in NO_x concentration due to the added dilution is strictly an effect of more dilution to the primary mixture. For CO, however, the final CO concentration is always a combined result of diluting the primary mixture and secondary-zone chemical reaction. This is because temperature has very little effect on CO destruction chemistry in the present model.

4. For secondary dilution to $\varphi_s = 0.5$, NO_x concentration is completely independent of secondary residence time. This is because of the suppression of NO_x reactions due to the low secondary zone reaction temperatures. For secondary dilution of rich primary mixtures to $\varphi_s = 0.7$, NO_x forms in the secondary zone due to chemical reaction. Therefore NO_x concentration increases with increasing secondary residence time for these rich primary mixtures only. Only in this region is chemical reaction important in the secondary zone. The final CO concentration always decreases with increasing secondary residence time because, in the present model, chemical reaction to destroy CO is not strongly affected by temperature.

5. Final NO_x and CO concentrations show negligible dependence on primary zone residence time.

6. Comparison of computed results with limited experimental data indicates that there is good agreement in trends between the idealized theoretical model and the experiment. The quantitative agreement steadily improves as the primary equivalence ratio increases. For the values of greatest interest ($\varphi_p \geq 1.4$) the agreement between theory and experiment is within ±50 percent. Apparently, effects of experimental heat transfer losses and mixing nonhomogeneity are less for these rich primary mixtures. These last two factors were not considered in the theoretical combustion model.

CONCLUDING REMARKS

This theoretical study reenforces the well-known idea that emissions of NO_x and CO can be reduced by two-stage combustion, burning rich in the primary zone and lean in the secondary. Our computations indicate that modest additional secondary dilution, from equivalence ratio 0.7 to 0.5, has a strong effect in reducing the absolute level of NO_x and CO concentrations. Also it was found that there is a large increase in NO_x formation due to a small amount (0.5 percent) of added FBN in the fuel. Our computed emission concentrations do not have a direct correlation with actual combustor emissions. However, the trends do indicate that removing only a moderate amount of the FBN from a real fuel during refining may not be sufficient to meet government emission standards.

Future synthetic fuels contain higher amounts of olefins and aromatic hydrocarbons than current petroleum fuels. The lower hydrogen/carbon ratio of the synthetic fuels will also affect pollutant formation. Therefore, we hope to perform additional computations using as the fuel a mixture of toluene (C_7H_8) and propane. The results for NO_x and CO emissions can then be compared with experimental flame tube results using the same fuel mixture.

REFERENCES

1 Pillsbury, P. W., et. al., "Investigative Com-
bustion Turbine Burner Performance with Coal Derived
Liquids Having High Fuel-Bound Nitrogen," ASME Paper
No. 78-GT-126, Apr. 1978.

2 Yamagishi, K., et. al., "A Study of NO_x Emis-
sion Characteristics in Two-Stage Combustion," Inter-
national Symposium on Combustion, 15th, Combustion
Institute, Pittsburgh, Pa., 1975, pp. 1157-1166.

3 Martin, F. J. and Dederick, P. K., "NO_x From
Fuel Nitrogen in Two-Stage Combustion," International
Symposium on Combustion, 16th, Combustion Institute,
Pittsburgh, Pa., 1977, pp. 191-198.

4 Takagi, T., Tatsumi, T., and Ogasawara, M.,
"Nitric Oxide Formation from Fuel Nitrogen in Staged
Combustion: Roles of HCN and NH_3," Combustion and
Flame, Vol. 35, No. 1, May 1979, pp. 17-25.

5 Bittker, D. A. and Scullin, V. J., "General
Chemical Kinetics Computer Program for Static and Flow
Reactions, with Application to Combustion and Shock-
Tube Kinetics," NASA TN D-6586, 1972.

6 Pratt, D. T., "PSR: A Computer Program for
Calculation of Steady-Flow Homogeneous Combustion Re-
action Kinetics," WSU-Bull.-336, Washington State
University, Pullman, Wash., 1974.

7 Jones, A. and Prothero, A., "The Solution of
the Steady-State Equations for an Adiabatic Stirred
Reactor," Combustion and Flame, Vol. 12, Oct. 1968,
pp. 457-464.

8 Bowman, C. T., "Kinetics of Pollutant Forma-
tion and Destruction in Combustion," Progress in
Energy and Combustion Science, Vol. 1, No. 1, 1975,
pp. 33-45.

9 Haynes, B. S., "Kinetics of Nitric Oxide Forma-
tion in Combustion," Alternative Hydrocarbon Fuels:
Combustion Kinetics, C. T. Bowman and J. Birkeland,
eds., American Institute of Aeronautics and Astron-
autics, New York, 1978, pp. 359-394.

10 Fenimore, C. P., "Formation of Nitric Oxide in
Premixed Hydrocarbon Flames," International Symposium
on Combustion, 13th, Combustion Institute, Pittsburgh,
Pa., 1971, pp. 373-380.

11 Jachimowski, C. J., "Analytical Study of Mech-
anisms for Nitric Oxide Formation During Combustion of
Methane in a Jet-Stirred Combustor," NASA TN D-8098,
1975.

12 Wakelyn, N. T., Jachimowski, C. J., and
Wilson, C. H., "Experimental and Analytical Study of
Nitric Oxide Formation During Combustion of Propane
in a Jet-Stirred Combustor," NASA TP-1181, 1978.

13 Anderson, D. N., "Effect of Premixing on
Nitric Oxide Formation," NASA TM X-68220, 1973.

14 Ceretto, L. S., "Modeling the Gas Phase
Kinetics of Fuel Nitrogen," WSS-CI Paper 76-12, Apr.
1976.

15 Olson, D. B. and Gardiner, W. C., "Combustion
of Methane in Fuel-Rich Mixtures," Combustion and
Flame, Vol. 32, No. 2, June 1978, pp. 151-161.

16 Wilson, W. E., Jr., "A Critical Review of the
Gas Phase Reaction Kinetics of the Hydroxyl Radical,"
Journal of Physical and Chemical Reference Data,
Vol. 1, No. 2, 1972, pp. 535-573.

17 Baulch, D. L., et. al., Evaluated Kinetic Data
for High Temperature Reactions, Vol. 1: Homogeneous
Gas Phase Reactions of the H_2-O_2 System, CRC Press,
Cleveland, O., 1972.

18 Hampson, R. F., Jr. and Garvin, D., eds.,
"Reaction Rate and Photochemical Data for Atmospheric
Chemistry, 1977," NBS-SP-513, National Bureau of
Standards, Washington, D.C., May 1978.

19 Schofield, K., "An Evaluation of Kinetic Rate
Data for Reactions of Neutrals of Atmospheric Inter-
est," Planetary and Space Science, Vol. 15, 1967,
pp. 643-670.

TABLE I. REACTION MECHANISM FOR PROPANE-AIR COMBUSTION

Reaction number	Reaction	Rate constant[a,b]			Reference
		A	n	θ	
1	$M + C_3H_8 \rightleftharpoons C_2H_5 + CH_3 + M$	5.0×10^{15}	0.0	32 713	12
2	$C_2H_5 \rightleftharpoons C_2H_4 + H$	3.16×10^{13}		20 483	12
3	$O + C_2H_4 \rightleftharpoons CH_3 + HCO$	2.26×10^{13}		1 359	12
4	$O + C_2H_4 \rightleftharpoons CH_2O + CH_2$	2.5×10^{13}		2 516	12
5	$CH_2 + O_2 \rightleftharpoons HCO + OH$	1.0×10^{14}		1 862	12
6	$CH_3 + C_3H_8 \rightleftharpoons CH_4 + C_3H_7$	2.0×10^{13}		5 184	12
7	$M + CH_4 \rightleftharpoons CH_3 + H + M$	4.7×10^{17}		46 900	15
8	$H + CH_4 \rightleftharpoons CH_3 + H_2$	1.26×10^{14}		5 989	12
9	$O + CH_4 \rightleftharpoons CH_3 + OH$	2.0×10^{13}		4 640	12
10	$OH + CH_4 \rightleftharpoons CH_3 + H_2O$	3.0×10^{13}		3 020	12
11	$CH_3 + O_2 \rightleftharpoons CH_2O + OH$	7.0×10^{11}		4 530	15
12	$CH_3 + O \rightleftharpoons CH_2O + H$	6.8×10^{13}		0.0	15
13	$CH_2O + H \rightleftharpoons HCO + H_2$	2.0×10^{13}		1 660	15
14	$CH_2O + O \rightleftharpoons HCO + OH$	5.0×10^{13}		2 300	15
15	$CH_2O + OH \rightleftharpoons HCO + H_2O$	5.0×10^{15}		6 540	15
16	$HCO + O \rightleftharpoons CO + OH$	3.0×10^{13}		0.0	15
17	$HCO + H \rightleftharpoons CO + H_2$	2.0×10^{13}		0.0	15
18	$HCO + OH \rightleftharpoons CO + H_2O$	3.0×10^{11}		0.0	15
19	$M + HCO \rightleftharpoons H + CO + M$	3.0×10^{14}		7 400	15
20	$CO + OH \rightleftharpoons CO_2 + H$	3.1×10^{11}		300	16
21	$M + CO + O \rightleftharpoons CO_2 + M$	2.8×10^{13}		-2 285	15
22	$CO + O_2 \rightleftharpoons CO_2 + O$	1.2×10^{11}		17 615	15
23	$H + O_2 \rightleftharpoons OH + O$	2.2×10^{14}		8 450	17
24	$O + H_2 \rightleftharpoons OH + H$	1.8×10^{10}	1.0	4 480	.
25	$H_2 + OH \rightleftharpoons H_2O + H$	5.2×10^{13}	.0	3 270	15
26	$O + H_2O \rightleftharpoons 2\ OH$	6.8×10^{13}	.0	9 240	17
27	$H + O_2 + M \rightleftharpoons HO_2 + M$	2.43×10^{15}	.0	-290	18
28	$M + O_2 \rightleftharpoons 2\ O + M$	1.9×10^{11}	.5	48 160	15
29	$M + H_2 \rightleftharpoons 2\ H + M$	2.2×10^{12}	.5	46 600	15
30	$H + OH + M \rightleftharpoons H_2O + M$	7.6×10^{23}	-2.6	0.0	15
31	$H + CH_3 \rightleftharpoons H_2 + CH_2$	2.7×10^{11}	.67	12 934	12
32	$O + CH_3 \rightleftharpoons OH + CH_2$	1.9×10^{11}	.68	12 934	12
33	$OH + CH_3 \rightleftharpoons H_2O + CH_2$	2.7×10^{11}	.67	12 934	12
34	$HO_2 + NO \rightleftharpoons NO_2 + OH$	2.0×10^{13}	0.0	1 200	18
35	$O + NO_2 \rightleftharpoons NO + O_2$	1.0×10^{13}		300	18
36	$NO + O + M \rightleftharpoons NO_2 + M$	9.4×10^{14}		-970	18
37	$NO_2 + H \rightleftharpoons NO + OH$	7.2×10^{14}		970	19
38	$O + N_2 \rightleftharpoons NO + N$	7.8×10^{13}		38 000	18
39	$N + O_2 \rightleftharpoons NO + O$	6.4×10^{9}	1.0	3 145	12
40	$N + OH \rightleftharpoons NO + H$	4.0×10^{13}	.0	0.0	12
41	$CH + N_2 \rightleftharpoons HCN + N$	1.5×10^{11}	.0	9 562	12
42	$CN + H_2 \rightleftharpoons HCN + H$	6.0×10^{13}	.0	2 669	12
43	$O + HCN \rightleftharpoons OH + CN$	1.4×10^{11}	.68	8 506	12
44	$OH + HCN \rightleftharpoons CN + H_2O$	2.0×10^{11}	.60	2 516	12
45	$CN + O_2 \rightleftharpoons NCO + O$	3.2×10^{13}	.0	505	12
46	$CN + CO_2 \rightleftharpoons NCO + CO$	3.7×10^{12}	.0	0.0	12
47	$H + NCO \rightleftharpoons NH + CO$	2.0×10^{13}	.0	0.0	12
48	$NH + OH \rightleftharpoons N + H_2O$	5.0×10^{11}	.5	1 006	12
49	$O + NCO \rightleftharpoons NO + CO$	2.0×10^{13}	.0	0.0	12
50	$N + NCO \rightleftharpoons N_2 + CO$	1.0×10^{13}		0.0	12
51	$CH + CO_2 \rightleftharpoons HCO + CO$	3.7×10^{12}		0.0	12
52	$C_3H_7 \rightleftharpoons C_2H_4 + CH_3$	4.0×10^{13}		16 658	12
53	$OH + C_2H_4 \rightleftharpoons H_2O + C_2H_3$	1.0×10^{14}		1 761	12
54	$H + C_2H_4 \rightleftharpoons H_2 + C_2H_3$	1.1×10^{14}		4 278	12
55	$CH + O_2 \rightleftharpoons HCO + O$	1.0×10^{13}		0.0	12
56	$M + C_2H_3 \rightleftharpoons C_2H_2 + H + M$	3.0×10^{16}		20 382	12
57	$O + C_2H_2 \rightleftharpoons CH_2 + CO$	5.2×10^{13}		1 862	12

[a] Rate constant is given by the equation $k = AT^n \exp(-\theta/T)$ where T is temperature in K and θ is the ratio of the reaction activation energy to the universal gas constant.

[b] Units of k for a unimolecular reaction are sec^{-1}; for a bimolecular reactions units are $cm^3/mole\ sec$ and for a termolecular reaction, units are $cm^6/mole^2\ sec$.

TABLE II. - COMPARISON OF CHEMICAL REACTION AND DILUTION EFFECTS

FOR MIXTURES WITH 1.0 PERCENT FBN

(a) Dilution to $\varphi_s = 0.7$.

φ_p	NO_x concentration, ppmm		
	Primary exhaust gas	Diluted primary exhaust gas	Secondary exhaust gas
0.8	2 302	2 019	2056
1.0	3 139	2 242	2291
1.2	1 146	690	801
1.4	627	327	447
	CO concentration, ppmm		
0.8	4 794	4 205	1415
1.0	19 589	13 992	2409
1.2	57 763	34 797	4579
1.4	96 213	50 111	5983

(b) Dilution to $\varphi_s = 0.5$.

φ_p	NO_x concentration, ppmm		
	Primary exhaust gas	Diluted primary exhaust gas	Secondary exhaust gas
0.8	2 302	1 466	1472
1.0	3 139	1 618	1628
1.2	1 146	498	505
1.4	627	237	244
	CO concentration, ppmm		
0.8	4 794	3 054	418
1.0	19 589	10 097	1002
1.2	57 763	25 114	1900
1.4	96 213	36 307	2545

Figure 2. - CO concentration versus primary equivalence ratio.

Figure 1. - NO$_x$ concentration versus primary equivalence ratio for propane-air.

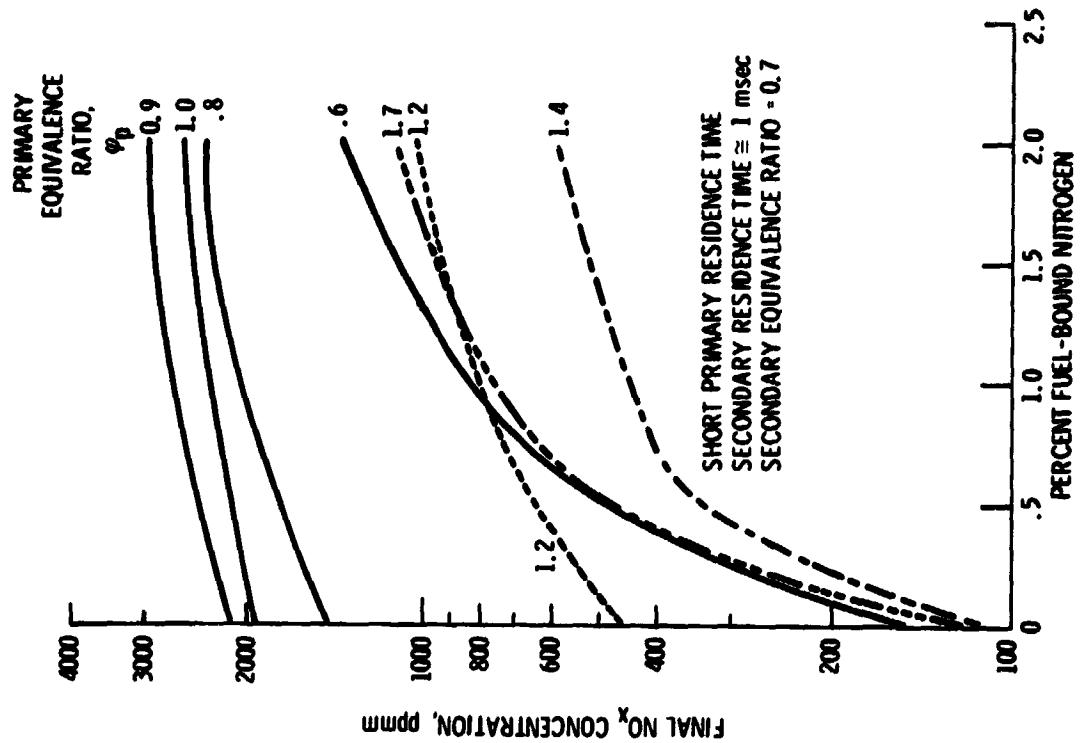Figure 4. - NO_x concentration versus primary equivalence ratio for additional secondary dilution.

Figure 3. - Effect of fuel-bound nitrogen on final NO_x concentration.

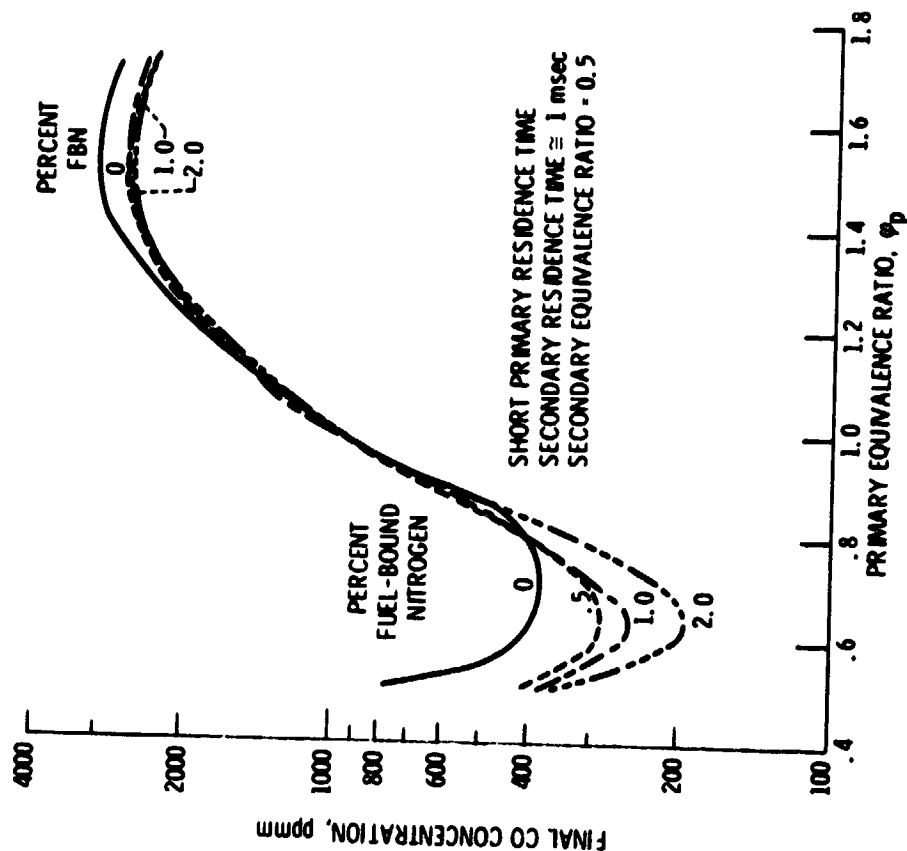Figure 5. – CO concentration versus primary equivalence ratio for added secondary dilution.

(a) NO_x CONCENTRATION.

Figure 6. – Effect of secondary dilution.

Figure 7. - Effect of secondary dilution on secondary reaction temperature.

SECOND-STAGE REACTION TEMPERATURE, K
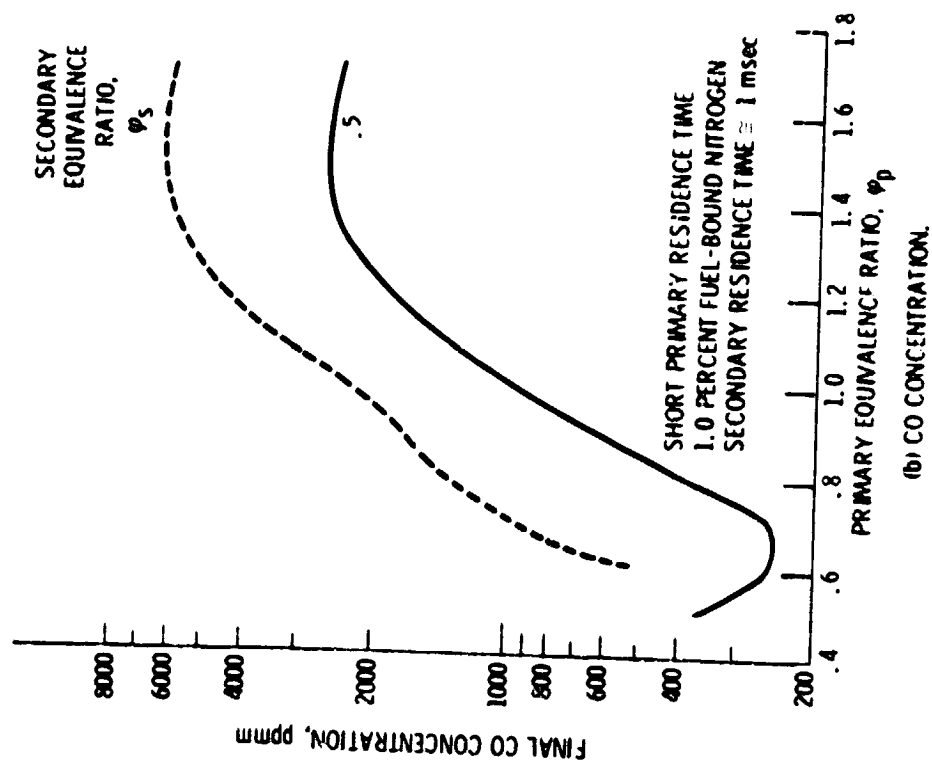
SECONDARY EQUIVALENCE RATIO, φ_s

0.7

SHORT PRIMARY RESIDENCE TIME
SECONDARY RESIDENCE TIME ≅ 1 msec
1.0% FUEL-BOUND NITROGEN

PRIMARY EQUIVALENCE RATIO, φ_p

.5

Figure 6. - Effect of secondary dilution.

(b) CO CONCENTRATION.

FINAL CO CONCENTRATION, ppmm

SECONDARY EQUIVALENCE RATIO, φ_s

SHORT PRIMARY RESIDENCE TIME
1.0 PERCENT FUEL-BOUND NITROGEN
SECONDARY RESIDENCE TIME ≅ 1 msec

PRIMARY EQUIVALENCE RATIO, φ_p

.5

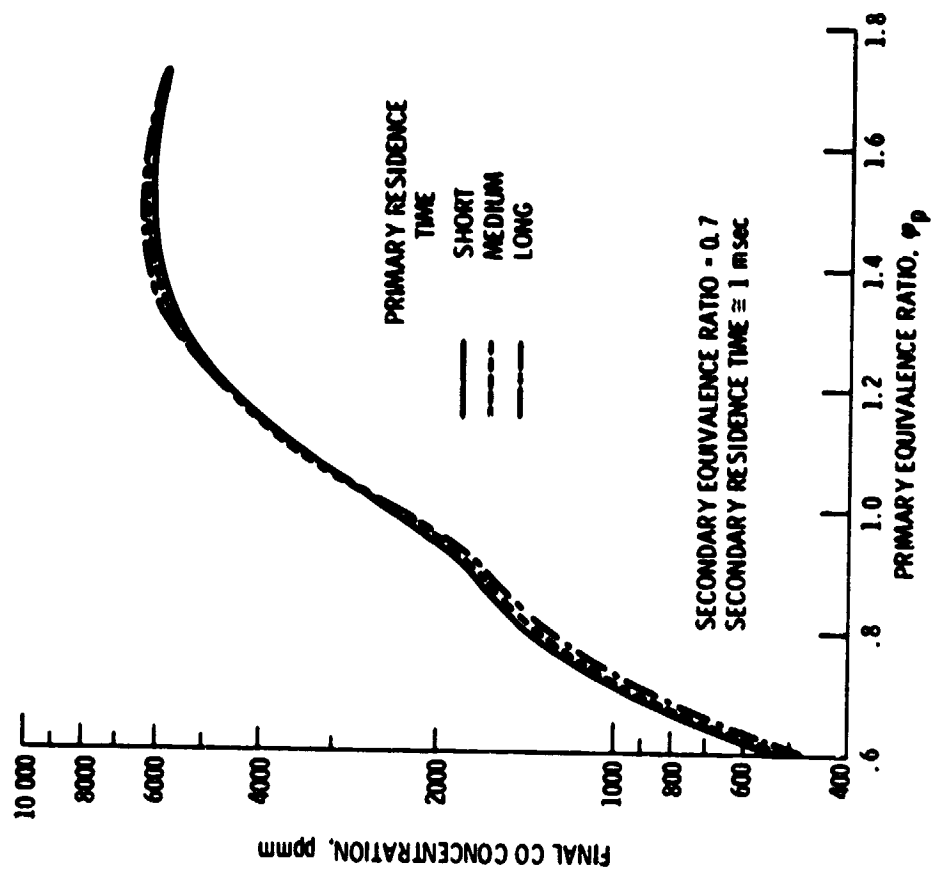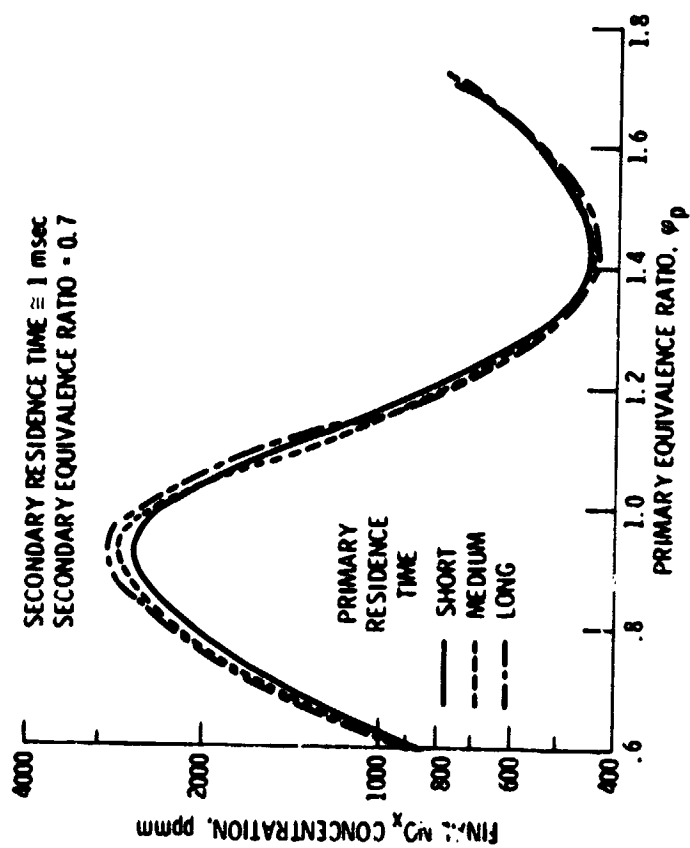Figure 8. – Effect of primary residence time on NO_x formation for 1.0 percent fuel-bound nitrogen content.
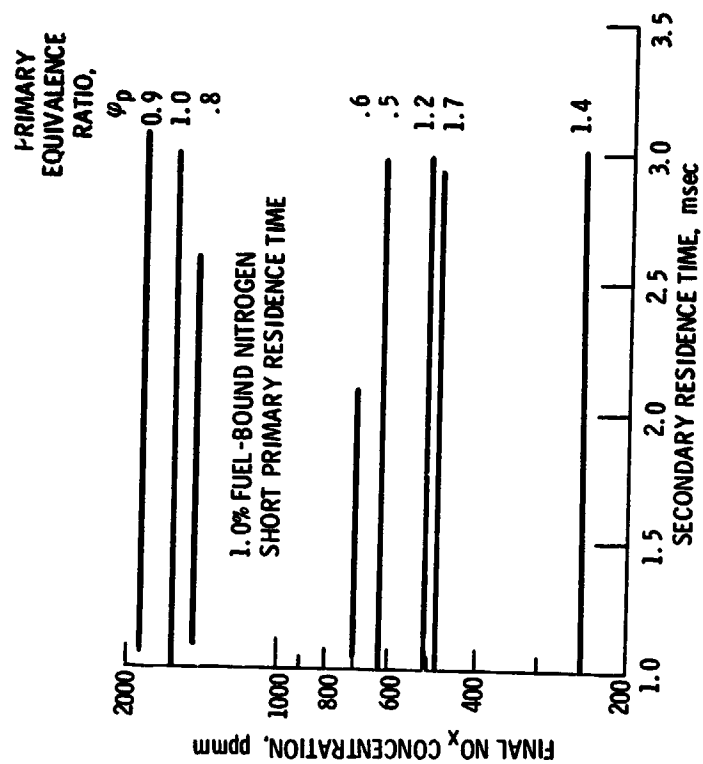

Figure 9. – Effect of primary residence time on CO formation for 1.0 percent fuel bound nitrogen content.

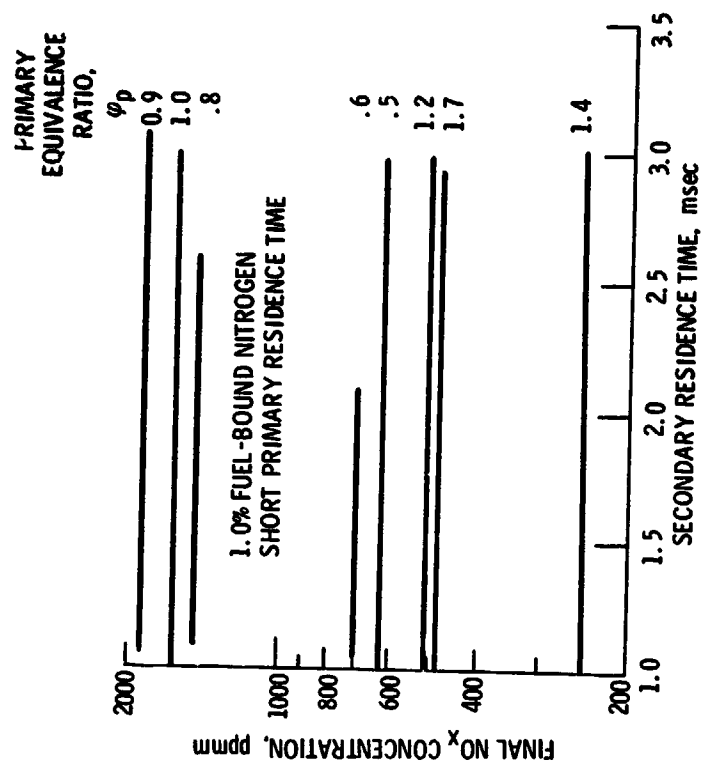PRIMARY EQUIVALENCE RATIO, φ_p

1.0% FUEL-BOUND NITROGEN
SHORT PRIMARY RESIDENCE TIME

FINAL NO_x CONCENTRATION, ppmm

SECONDARY RESIDENCE TIME, msec

(b) SECONDARY EQUIVALENCE RATIO = 0.5.

Figure 10. - Effect of secondary residence time on final NO_x concentration.

PRIMARY EQUIVALENCE RATIO, φ_p

1.0% FUEL-BOUND NITROGEN
SHORT PRIMARY RESIDENCE TIME

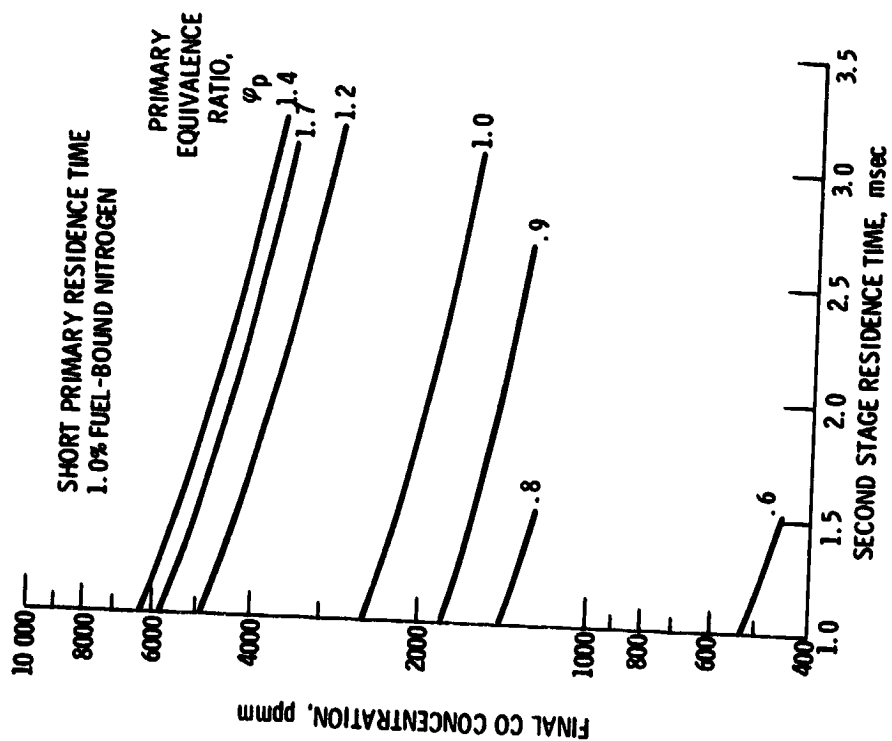FINAL NO_x CONCENTRATION, ppmm

SECOND STAGE RESIDENCE TIME, msec

(a) SECONDARY EQUIVALENCE RATIO = 0.7.

Figure 10. - Effect of second stage residence time on final NO_x concentration.

PRIMARY EQUIVALENCE RATIO, φ_p
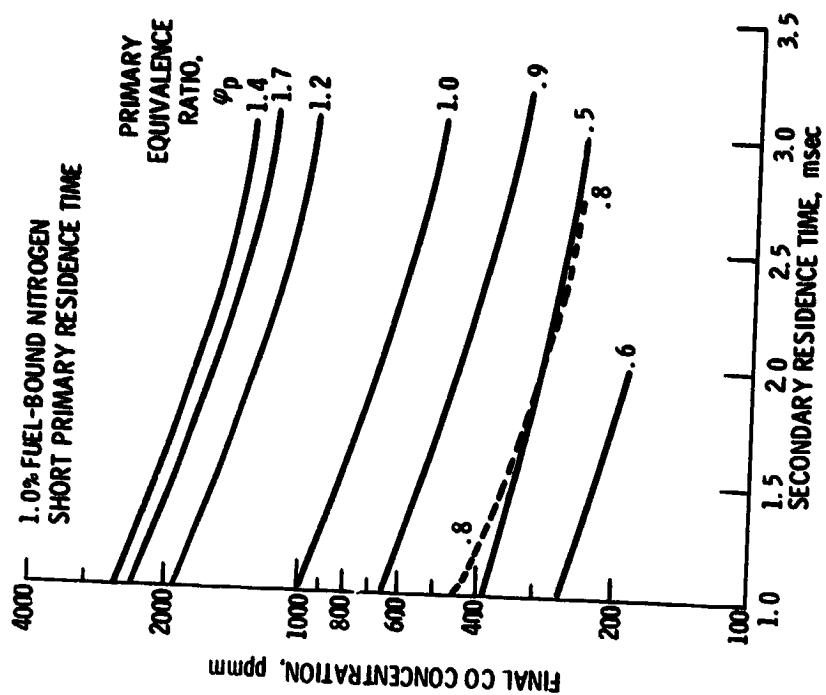
1.0% FUEL-BOUND NITROGEN
SHORT PRIMARY RESIDENCE TIME

1.4
1.7
1.2
1.0
.9
.8
.5
.8
.6

FINAL CO CONCENTRATION, ppmm

SECONDARY RESIDENCE TIME, msec

(b) SECONDARY EQUIVALENCE RATIO = 0.5.

Figure 11. - Effect of secondary residence time on final CO concentration.

SHORT PRIMARY RESIDENCE TIME
1.0% FUEL-BOUND NITROGEN

PRIMARY EQUIVALENCE RATIO, φ_p

1.4
1.7
1.2
1.0
.9
.8
.6

FINAL CO CONCENTRATION, ppmm

SECOND STAGE RESIDENCE TIME, msec

(a) SECONDARY EQUIVALENCE RATIO = 0.7.

Figure 11. - Effect of second-stage residence time on final CO concentration.
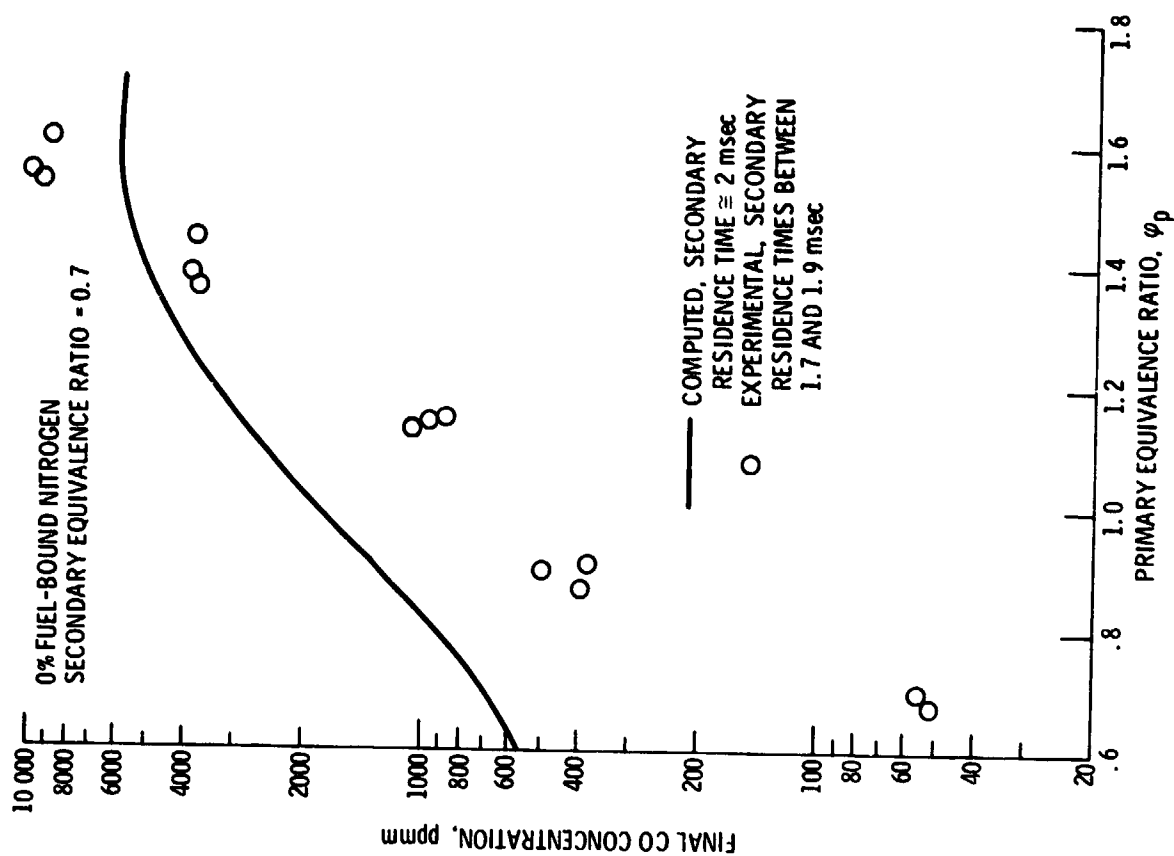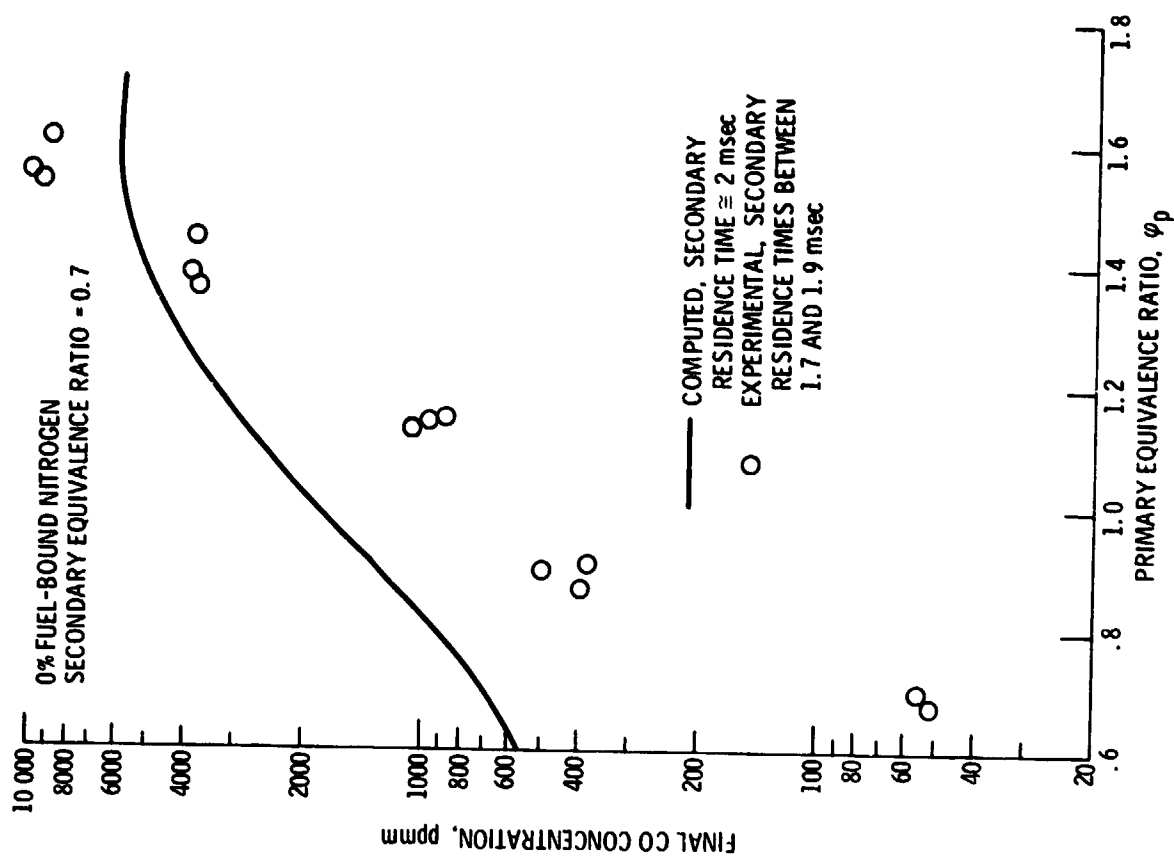
Figure 13. – Comparison of computed and experimental CO concentrations.

Figure 12. – Comparison of computed and experimental NO$_x$ concentrations.